

## Electric field gradients in Au-Te alloys and charge transfer in some intermetallic compounds of nontransition metals with gold

T. K. Sham, R. E. Watson, and M. L. Perlman  
*Brookhaven National Laboratory, Upton, New York 11973*  
 (Received 23 February 1979)

This work is an extension of an earlier study of charge transfer occurring when Au is alloyed with nontransition (main-group) elements. Au Mössbauer-isomer-shift and quadrupole-splitting results are reported for a series of Au-Te alloys: AuTe<sub>2</sub>, Au<sub>0.12</sub>Te<sub>0.88</sub>, Au<sub>0.052</sub>Te<sub>0.948</sub>, and Au<sub>0.01</sub>Te<sub>0.99</sub>. Asymmetric doublets are observed in the <sup>197</sup>Au Mössbauer spectra of these alloys and are attributed to the Goldanskii-Karyagin effect. The sign of the electric field gradient is deduced to be negative. The quadrupole splittings, substantial relative to those ordinarily encountered in metals, are consistent with the presence of an amount of bonding charge along nearest-neighbor Te-Au-Te lines which exceeds by about 0.1e the charge along the two longer Te-Au-Te axes defining the equatorial positions in the distorted Te octahedron. The net charge transfer,  $\delta$ , in AuTe<sub>2</sub> and in related AuM<sub>2</sub> compounds—compounds of common composition but not common structure—has been evaluated with a modified model which includes photoelectron binding-energy shifts, isomer shifts, and volume-correction terms at both the Au and M sites. With an extension of this model, an attempt is made to reduce the extent of uncertainty arising from reference-level shifts in the analysis of photoelectron data: the net charge transfer is assumed to be a linear function of the chemical-potential difference between the alloying species. As has been found previously, the analysis provides evidence for *d*-non-*d* charge compensation. That is, at Au sites a decrease in *d* count accompanies a net gain,  $\delta$ , in charge. The extended model yields  $\delta$  values which vary more smoothly than those obtained previously and show a trend consistent with general chemical behavior. Finally, while the full analysis indicates a gain of charge at Au sites and charge loss at the metalloid sites in AuSn<sub>2</sub>, AuSb<sub>2</sub>, and AuTe<sub>2</sub>, the Mössbauer isomer-shift data for the metalloids actually indicate that *s* charge increases in Te, though it decreases in the cases of Sn and Sb. This, taken with the net-charge-flow estimates, suggests a systematic variation in the relative loss of *s* vs *p* charge across the AuSn<sub>2</sub>-AuSb<sub>2</sub>-AuTe<sub>2</sub> sequence. Energy differences associated with these *s,p* effects are significant in relation to the heats of formation of these compounds.

### I. INTRODUCTION

Recently we reported<sup>1</sup> a study of charge transfer which takes place when gold is alloyed with nontransition (main-group) metals. Results of that work were based on Au-site Mössbauer-isomer-shift and core-electron-photoemission data. In this paper we extend the analysis to consider the Au-site quadrupole splittings observed in the Mössbauer spectra of the Au-Te alloys. Furthermore, we incorporate metalloid as well as Au-site data in the calculation of charge transfer for a set of AuM<sub>2</sub> (*M* = Al, Ga, In, Sn, Sb, and Te) compounds of like composition. Previously inferred trends in Au-site charge transfer are confirmed, but consideration of the Au quadrupole splittings, which provide a measure of the asphericity of bonding charge, with consideration of the metalloid site shifts, provides a more complete picture of the bonding between main-group elements and Au, a metal with chemically active *d* bands.

Some details of the experiments are given in Sec.

II. The electric field gradients in Au-Te and what they indicate concerning the asphericity of bonding charge surrounding Au sites are considered in Sec. III. This is sometimes discussed<sup>2</sup> in terms of free-atom Au-6*p* orbital charge. Such charge extends far out into the lattice; we have, instead, dealt with 6*p* charge normalized within a Au atomic site. This provides, we believe, a more reasonable basis for describing such bonding effects. Analysis of quadrupole effects requires knowledge of the sign of the splitting, which is inferred from the asymmetries observed in the spectra and their attribution to the Goldanskii-Karyagin effect<sup>3</sup> (Sec. IV). Charge transfer is dealt with in Sec. V. A standard problem in the treatment<sup>1,4,5</sup> of photoemission data is caused by shifts in the Fermi level, with respect to which core-level energies are measured. We have, for the first time, attempted to reduce the difficulty associated with this by assuming that the charge transfer  $\delta$  is linearly related to a difference in chemical potentials. This is done in Sec. VI. In the analyses of Secs. V

and VI, contributions to the measured binding-energy shifts due to changes in extra-atomic screening of the final-state hole are neglected. In addition, the Madelung-like contribution to the potential, due to any net charge transfer was not defined in detail. These matters are dealt with in Sec. VII. Conclusions are presented in Sec. VIII.

## II. EXPERIMENTS AND RESULTS

Au-Te intermetallic alloys were prepared in fused silica tubes under vacuum and were quenched rapidly from the melt to room temperature.  $\text{AuTe}_2$  was annealed and was shown to have monoclinic structure by the x-ray powder method. The eutectic composition,  $\text{Au}_{0.12}\text{Te}_{0.88}$ , showed a more complicated powder pattern, essentially a superposition of those of  $\text{AuTe}_2$  and Te. The more dilute alloys,  $\text{Au}_{0.052}\text{Te}_{0.948}$  and  $\text{Au}_{0.011}\text{Te}_{0.989}$ , showed patterns similar to that of the eutectic, albeit with different intensity ratios. Au is at most only slightly soluble<sup>6</sup> in Te, and how much Au-Te solution may have been present, perhaps metastably, in the dilute compositions is not known. Mössbauer spectra of  $^{197}\text{Au}$  in these systems were obtained with source and absorbers at liquid-helium temperature. All samples were ground into very fine powders ( $\sim 200$  mesh) which were mixed with lucite and subsequently pressed into disks. In one experiment, very fine sample powder was dropped from a pipette into a lucite sample holder to determine whether orientation effects due to pressing and the texture of the sample were significant. No appreciable difference in Mössbauer parameters was observed from the different sample preparations. Results are given in Table I and representative spectra are shown in Fig. 1. It appears that all the Au-Te

TABLE I. Mössbauer parameters for Au-Te alloys.

Alloy	IS ( $\text{mm s}^{-1}$ ) <sup>a</sup>	QS ( $\text{mm s}^{-1}$ ) $= \frac{1}{2}e^2qQ$
$\text{AuTe}_2$	2.16	2.29
$\text{Au}_{0.12}\text{Te}_{0.88}$	2.36	2.13
$\text{Au}_{0.052}\text{Te}_{0.948}$	2.24	2.17
$\text{Au}_{0.011}\text{Te}_{0.989}$	2.1(3)	2.1(3)
$\text{Au}_{<0.002}\text{Te}_{>0.998}$	1.9(3)	...

<sup>a</sup>The isomer shift (IS) is relative to an enriched Pt source; errors are  $\pm 0.05 \text{ mm s}^{-1}$  except specified.

<sup>b</sup>This spectrum is poor in quality due to weak absorption. Values have been extracted from a broad, asymmetric, barely resolved pattern.

<sup>c</sup>Emission spectrum from P. H. Barrett *et al.*, J. Chem. Phys. **39**, 1033 (1963). Quadrupole splitting (QS) was not reported.

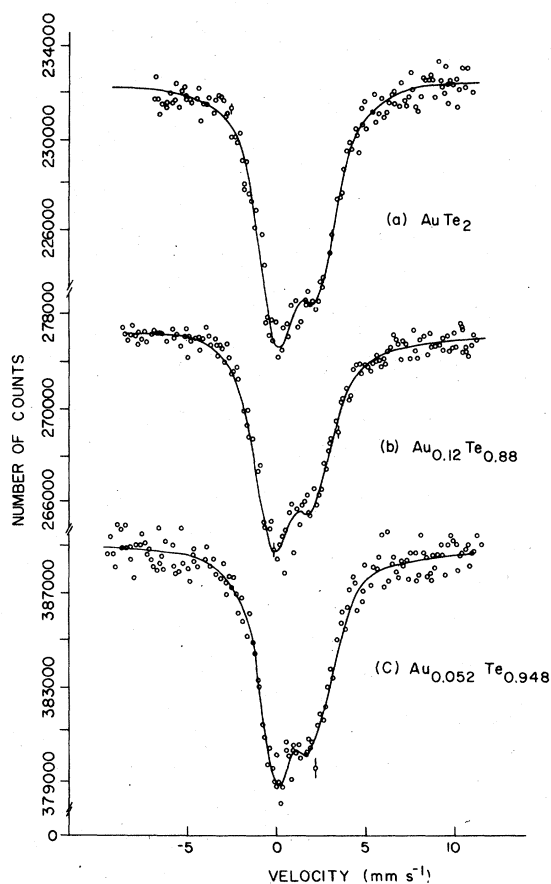


FIG. 1. Mössbauer spectra of some Au-Te alloys.

alloys exhibit almost constant isomer shift and quadrupole splitting. This is consistent with the suggestion made earlier<sup>1</sup> that the local order in even the most dilute of these alloy systems is very similar to that of the corresponding compounds.

Core-electron binding-energy shifts were measured using a Varian and an ADES 400 spectrometer with  $\text{Mg } K\alpha$  x rays. Au 4*f* levels in pure Au served for calibration. The Au-shift results have been reported previously<sup>1</sup> but Au in  $\text{AuAl}_2$  was remeasured because of discrepancies in the previously reported values.<sup>1</sup> Some Mössbauer isomer shifts are from the literature.<sup>7-9</sup>

## III. ELECTRIC FIELD GRADIENTS IN Au-Te

The structures<sup>10</sup> of  $\text{AuTe}_2$  have been known for a long time. Except for the metastable cubic phase,<sup>11</sup> which can be prepared only by rapid quenching,<sup>11</sup> all  $\text{AuTe}_2$  structures, whether occurring in nature or prepared in the laboratory, are characterized, essen-

tially, by distorted six coordinated environments at both Au and Te sites. In the monoclinic calaverite structure<sup>10</sup> Au is at the center of a distorted octahedron with two axial tellurium neighbors at 2.68 Å and four equatorial ones at 2.97 Å. It is apparent that this distortion would give rise to quadrupole splitting in the Au Mössbauer spectrum. Substantial splittings ( $\sim 2 \text{ mm s}^{-1}$ ) are indeed observed in AuTe<sub>2</sub> and in the more dilute alloys. It is very interesting to note that the electric field gradient  $eq = -4 \times 10^{18} \text{ V/cm}^2$ , derived from the splitting,  $2 \text{ mm s}^{-1}$ , and the assumed value  $Q_{\text{Au}} = 0.594 \text{ b}$  is considerably larger than what is normally observed in noncubic metallic systems.<sup>12</sup>

The  $eq$  observed in AuTe<sub>2</sub> can be expressed as a sum of two contributions,

$$eq(\text{AuTe}_2) = (1 - R)eq_{\text{val}} + (1 - \gamma_{\infty})eq_{\text{latt}}, \quad (1)$$

where  $R$  and  $\gamma_{\infty}$  are Sternheimer factors.<sup>13</sup>  $(1 - R)$  is close to unity and  $\gamma_{\infty} = -65$  for Au.<sup>14</sup>  $eq_{\text{val}}$  arises from the noncubic valence charge distribution at the Au site, which may be enhanced by Au-Te covalent mixing. The  $(1 - \gamma_{\infty})eq_{\text{latt}}$  term, the lattice contribution, is small, as may be expected for metallic systems.<sup>15</sup>

The sign of  $\frac{1}{2}e^2qQ$  in AuTe<sub>2</sub> is negative, as obtained from the asymmetry in the splitting to be discussed in Sec. IV. The sign of  $eq_{\text{val}}$  is thus negative because  $Q_{\text{Au}}$  is positive. A negative field gradient,  $q_{\text{val}}$ , implies that there is more electron density along the  $z$  axis of the field gradient, the linear Te-Au-Te axis, than in the plane in which there are the four Te atoms at a longer distance. Consider, for the moment, the implications of assuming that the quadrupole splitting arises from an excess Au- $6p$  charge along the  $z$  axis. Normalizing<sup>16</sup> the  $6p$  electron to the Au atomic cell produces a  $\langle r^{-3} \rangle_{6p}$  integral of  $\sim 25$  a.u. and, with this, one finds that the observed splitting is equivalent to a charge excess of  $0.1e$  in the pair of bonds involving  $p_z$  orbital character as compared with either  $p_x$  or  $p_y$ . This is not inconsistent with the net increase  $\sim 0.2e$  in  $s$  and  $p$  charge at the Au site, which has been inferred<sup>1</sup> previously. Similarly, if only  $5d$  charge is considered, an excess of  $d$  charge of  $0.25e$  along the  $z$  axis would yield the observed splitting. Since Au- $5d$  character is lost by hybridization with Te this might be viewed as an increased depletion in the  $x-y$  plane. The picture which emerges is a modest excess of  $5d-6p$  bonding charge along the  $z$  axis. This then involves charge in the Te sites as well, whose contributions to  $eq$  are not included in the above charge estimates. If one takes both Au and Te sites into account, the quadrupole splitting indicates an excess of  $(0.1 \pm 0.05)e$  charge in the axial bonds, a result which is consistent with previous observations.<sup>2,17</sup>

#### IV. GOLDANSKII-KARYAGIN ASYMMETRY

All Au-Te alloys of this study show pronounced asymmetric doublets in the Mössbauer spectra of their random powder samples (Fig. 1). The relative intensity of the components of the doublet for AuTe<sub>2</sub>, i.e., area of higher-velocity peak divided by area of lower-velocity peak, is estimated, with the spectrum fitted to Lorentzian line shapes having slightly different widths, to be  $0.91 \pm 0.05$ . This asymmetry can be due to several effects: presence of impurity, magnetic relaxation, and vibronic anisotropy. An x-ray powder diffraction pattern of the well annealed AuTe<sub>2</sub> shows that it is monoclinic, consistent with previously reported results,<sup>10</sup> and suggests that it is very unlikely that the asymmetry arises from impurity or presence of a second phase. The contribution of magnetism can also be ruled out since AuTe<sub>2</sub> is diamagnetic. We are left with the vibronic anisotropy. It must be emphasized that because the splitting observed here is comparable to the width of the peaks, the fitted area ratio has a large uncertainty and is at best semiquantitative. What is important is that the ratio is less than unity. Similar asymmetry of quadrupole doublets has been documented in iron,<sup>18</sup> tin,<sup>19</sup> and tellurium<sup>20</sup> compounds and also in Au(CN)<sub>2</sub><sup>-</sup>.<sup>17</sup> These effects have been attributed by Goldanskii and Karyagin to the anisotropy of the Debye-Waller factor associated with atomic vibrations. In cases such as <sup>57</sup>Fe, <sup>119</sup>Sn, and <sup>125</sup>Te, it has been shown<sup>18-20</sup> that the ratio of the areas of the two lines,  $R = A(\frac{3}{2})/A(\frac{1}{2})$ , depends upon the difference  $\langle z^2 \rangle - \langle x^2 \rangle$ , where  $\langle z^2 \rangle$  and  $\langle x^2 \rangle$  are the mean-square vibrational amplitudes parallel and perpendicular, respectively, to the  $z$  electric-field-gradient axis. When  $\langle z^2 \rangle > \langle x^2 \rangle$ , then  $R < 1$ ; if  $\langle z^2 \rangle < \langle x^2 \rangle$ , then  $R > 1$ . This can be used in two ways: if  $\langle z^2 \rangle - \langle x^2 \rangle$  is known, it can be used to calculate  $R$ ; and qualitatively, if the sign of  $\langle z^2 \rangle - \langle x^2 \rangle$  is known,  $R$  can be used to determine the sign of the quadrupole splitting. In the <sup>197</sup>Au case, the situation is complicated by the  $E2-M1$  mixed multipolarity of the  $I_{1/2} \rightarrow I_{3/2}$  Mössbauer transition.<sup>17</sup> In a noncubic axially symmetric environment, the ratio of the intensities of the two lines can be expressed<sup>17</sup> as

$$R(\theta, \delta_{\gamma}) = \frac{A(3/2)}{A(1/2)} = \frac{2(\sqrt{3} + \delta_{\gamma})^2 - 3(1 + 2\sqrt{3}\delta_{\gamma} - \delta_{\gamma}^2) \sin \theta}{2(1 - \sqrt{3}\delta_{\gamma})^2 + 3(1 + 2\sqrt{3}\delta_{\gamma} - \delta_{\gamma}^2) \sin \theta}, \quad (2)$$

where  $\theta$  is the angle between the axis of the electric field gradient and the axis of the Mössbauer spectrometer, and  $\delta_{\gamma}$  is the  $E2/M1$  mixing ratio of the 77-keV transition. If we set  $\delta_{\gamma} = 0$  in Eq. (2), include

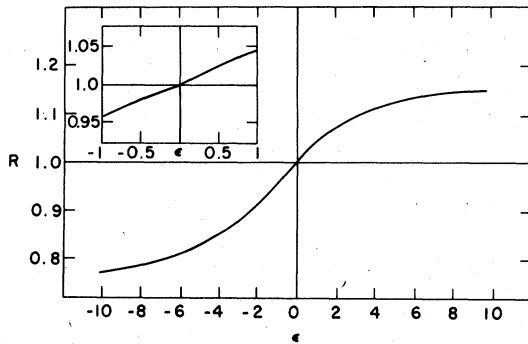


FIG. 2. Intensity ratio,  $R = A_{3/2}/A_{1/2}$ , of the two components of the quadrupole split 77-keV  $^{197}\text{Au}$  Mössbauer line as a function of the vibrational asymmetry parameter  $\epsilon$  (see text).

the Debye-Waller asymmetry, and take into account the fact that the sample is randomly oriented powder, we have

$$R_{\text{powder}} = \frac{A(3/2)}{A(1/2)} = \frac{\int_0^1 (1 + \mu^2) e^{-\epsilon \mu^2} d\mu}{\int_0^1 (5/3 - \mu^2) e^{-\epsilon \mu^2} d\mu}, \quad (3)$$

where  $\mu = \cos\theta$ ,  $\epsilon = (1/\lambda^2)(\langle z^2 \rangle - \langle x^2 \rangle)$ , and  $\lambda$  is  $1/2\pi$  times the Mössbauer-photon wavelength. This expression is identical to the equation applied to the  $^{57}\text{Fe}$ ,  $^{119}\text{Sn}$ , and  $^{125}\text{Te}$  quadrupole splittings. In the  $^{197}\text{Au}$  case, Prosser *et al.*<sup>17</sup> have measured  $\delta_v$  to be  $-0.352$ , and for random Au containing absorbers we have

$$R_{\text{powder}} = \frac{A(3/2)}{A(1/2)} = \frac{\int_0^1 (a - \mu^2) e^{-\epsilon \mu^2} d\mu}{\int_0^1 (b + \mu^2) e^{-\epsilon \mu^2} d\mu}, \quad (4)$$

where  $a$  and  $b$  are constants obtained by substituting the value  $-0.352$  for  $\delta_v$  in Eq. (2). Numerical analysis of Eq. (4) (Fig. 2) shows that if  $\langle z^2 \rangle > \langle x^2 \rangle$  ( $\epsilon$  positive), then  $R > 1$ ; if  $\langle z^2 \rangle < \langle x^2 \rangle$  ( $\epsilon$  negative), then  $R < 1$ , in contrast to what one would expect in the  $^{57}\text{Fe}$ ,  $^{119}\text{Sn}$ , and  $^{125}\text{Te}$  cases. In  $\text{Au}(\text{CN})_2^-$ ,  $eq$  is known to be negative and  $R$  observed from a random sample is less than unity. This observation immediately indicates that  $\epsilon$  is negative in  $\text{Au}(\text{CN})_2^-$ .<sup>17</sup> In  $\text{AuTe}_2$ , because its local structure is similar to that of  $\text{Au}(\text{CN})_2^-$ , one expects that  $\epsilon$  should be negative. Consequently we have  $R < 1$ , meaning that the less intense line at positive velocity in Fig. 1 has identity  $I_{3/2}$ . Thus the quadrupole splitting at the Au site is negative and the electric field gradient  $eq$  is negative. A negative  $eq$  at Au in  $\text{AuTe}_2$  is entirely consistent with previous experience<sup>2,17</sup> and with the binding-energy shift arguments discussed in Sec. V. The determination of sign of  $eq$  from the asymmetry is illustrated in Table II.

TABLE II. Summary of the sign of  $^{57}\text{Fe}$  and  $^{197}\text{Au}$  Mössbauer quadrupole splittings determined by Goldanskii-Karyagin asymmetry (see text).<sup>a</sup>

	$R = \frac{A(3/2)}{A(1/2)}$	$\epsilon = \frac{1}{\lambda^2}(\langle z^2 \rangle - \langle x^2 \rangle)$	QS <sup>c</sup>
$^{57}\text{Fe}^b$	$>1$	-	+
	$<1$	+	-
$^{197}\text{Au}$	$>1$	+	+
	$<1$	-	-

<sup>a</sup>Note that in  $^{57}\text{Fe}$ , the ground state is  $I = \frac{1}{2}$  and the excited state (14.4 keV) is  $I = \frac{3}{2}$ , whereas in  $^{197}\text{Au}$  the ground state is  $I = \frac{3}{2}$  and the excited state (77 keV) is  $I = \frac{1}{2}$ .

<sup>b</sup>The  $^{57}\text{Fe}$  case also applies to  $^{119}\text{Sn}$  and  $^{125}\text{Te}$ .

<sup>c</sup>QS =  $\frac{1}{2}e^2qQ$ ;  $Q$  is the nuclear quadrupole moment and is positive in both  $^{57}\text{Fe}$  and  $^{197}\text{Au}$  cases.

## V. CHARGE TRANSFER IN $\text{Au}M_2$ ( $M = \text{Al, Ga, In, Sn, Sb, Te}$ )

In a previous paper<sup>1</sup> we have shown that from the Au core-level binding-energy shift  $\Delta E_{\text{Au}}$ , which is associated with alloying, we can estimate the net charge flow,  $\delta$ , to or from the Au site. The procedure is not straightforward because, in order to evaluate charge flow from the measurement, one needs to know from theory the core-electron binding-energy shift per unit valence charge change at the site. This theoretical quantity refers to the photoemitted core electron being removed to infinity, whereas the measurement is referred to the Fermi level. Furthermore, because more than one kind of valence charge is usually involved in alloying,  $d$  and non- $d$  of Au for example, there is an interplay of terms associated with charge redistribution. In addition, alloying of an element may introduce modification in the volume attributed to an atomic site and may modify the ability of the medium to screen the final-state hole created by photoemission. In the previous paper, estimates of alloy site charging are based on the Au core-level shifts alone. As will be shown below, some of the difficulties in this problem are reduced by utilization of shift data for both constituents in the binary alloys.

Although the analysis is numerically complicated and requires estimation of some quantities, the results do indicate the magnitude and nature of valence charge modification upon alloying.

If, for the moment, final-state screening is neglected, the measured Au-site binding-energy shift is written

$$\Delta E_{\text{Au}} = +(\phi_{\text{Au}} - \phi_M - \Delta\phi) - \Delta n_c F(\text{cond}) - \Delta n_d F(d) + \delta F(\text{latt}) + \left( \frac{dE}{dV} \Delta V \right)_{\text{Au}}, \quad (5)$$

where  $\delta$  is the sum of  $d$  and conduction electron count changes associated with the Au atom,

$$\delta \equiv \Delta n_c + \Delta n_d \quad (6)$$

One can similarly estimate the charge flow in terms of a metalloid-site core-electron binding-energy shift

$$\Delta E_M = -\Delta\phi - \Delta n_s F_s - \Delta n_p F_p - \frac{\delta}{2} F_{\text{latt}} + \left( \frac{dE}{dV} \Delta V \right)_M \quad (7)$$

where

$$-\frac{\delta}{2} = \Delta n_s + \Delta n_p \quad (8)$$

and  $\Delta n_s$  and  $\Delta n_p$  are changes in  $s$  and  $p$  counts on the metalloid atom. The minus sign for  $\delta$  and the factor of  $\frac{1}{2}$  follow because  $\delta$  is defined by Eq. (6) in terms of the Au site and because there are two equivalent metalloid atoms per Au atom in these compounds.

$F_s$ ,  $F_p$ ,  $F(\text{cond})$ , and  $F(d)$  of Eqs. (5) and (7) are the changes in core-electron binding energies<sup>21</sup> associated with the removal of a single valence electron from the atomic site in question. This definition leaves the  $F$ 's as positive quantities much like Coulomb integrals. Now, the addition or removal of a valence electronic charge causes the other valence and core electrons to relax; the effect of this relaxation is included in the estimation of  $F$ , causing the value to be smaller in magnitude than the direct Coulomb interaction between a valence and core electron. For these estimates valence electron orbitals were normalized to the atomic Wigner-Seitz cell.

Charge at an atomic site necessitates a compensating charge in the surrounding lattice and the  $F_{\text{latt}}$  and  $F(\text{latt})$  terms are the spherical Madelung-like potential energies associated with a unit charge displaced out into the lattice surrounding a metalloid site and Au site, respectively. The positive sign of  $F(\text{latt})$ , Eq. (5), follows from the fact that the charge displaced into the lattice is opposite in sign to the Au-site charge  $\delta$ . We use here values estimated after the manner employed previously<sup>1</sup>; more will be said concerning this in Sec. VII. The terms  $(dE/dV)\Delta V$  are calculated binding-energy changes associated with the difference between the volume assignable to an atom in the alloy or compound and the volume the atom occupies as a pure element. Vegard's law approximately describes the behavior of the compounds of concern here—their molecular volumes equal the sum of the pure element atomic volumes. Deviations from Vegard have been accounted for by scaling both metalloid and Au-site volumes according to the ratio  $V(\text{Au}M_2)/[V(\text{Au}) + 2V(M)]$ . The same scaled volumes are used to obtain volume-corrected estimates<sup>22</sup> of metalloid  $\Delta n_s$  values and Au  $\Delta n_c$  values from Mössbauer isomer shifts. Finally, a binding-energy shift is measured with respect to the Fermi level  $\epsilon_F$  of the sample, while the above  $F$  terms are calculated with respect to the zero of the crystal potential energy within the sample. The first terms of Eqs. (5) and (7) account for any shift in  $\epsilon_F$  with respect to the crystal zero, i.e., any shift of the internal chemical potential. This is illustrated in Fig. 3:  $\Delta\phi$  is the shift on going from the metalloid to the

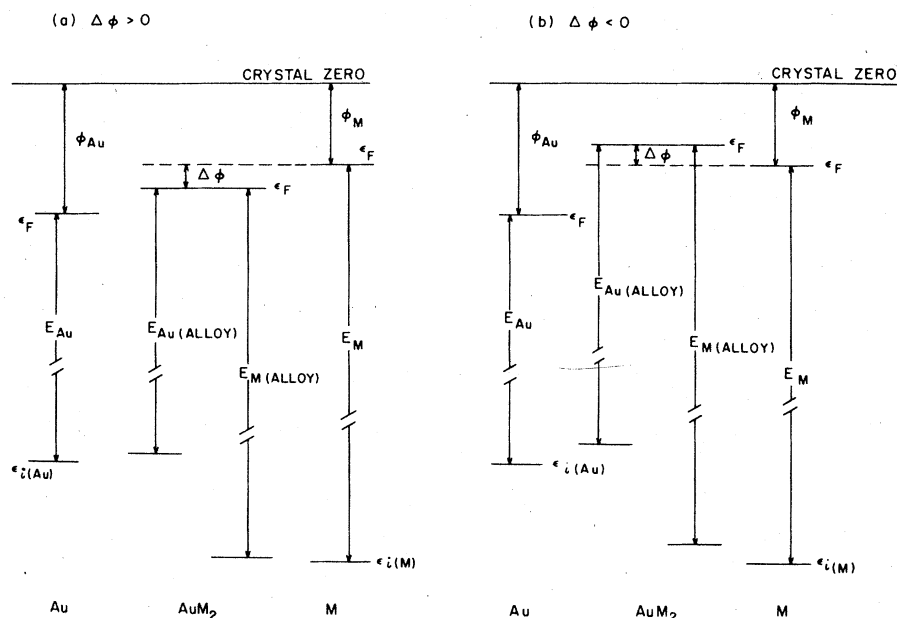


FIG. 3. Energy levels involved in core-electron photoemission and the definition of  $\Delta\phi$ , the Fermi-level shift of the alloy,  $\text{Au}M_2$ , with respect to the pure metalloid,  $M$ .

TABLE III. Data relevant to Eqs. (5)–(9). Refer to text.

core level		Metalloid			Au				
		$\phi^b$ (Work functions) (eV)	$\phi^c$ [Pauling (scaled)] (eV)	$\Delta n_s^d$	$F_p - F_{latt}$ (eV)	$\Delta E(\text{core})^d$ (eV)	$\Delta n_c^d$	$\Delta E(4f)^d$ (eV)	$F(d) - F(\text{latt})$ (eV)
Al	2p	4.20	3.86	... <sup>a</sup>	6.5	+0.9	0.65	+1.8	
Ga	3p	4.10	4.08	... <sup>a</sup>	5.5	+0.5	0.50	+1.3	
In	3d	3.90	4.30	... <sup>a</sup>	4.8	+0.3 <sub>0</sub>	0.40	+0.71	
Sn	3d	4.15	4.51	-0.04	5.3	+0.8 <sub>0</sub>	0.33	+1.32	
Sb	3d	4.40	4.73	-0.02	5.6	-0.1 <sub>0</sub>	0.27	+0.22	
Te	3d	4.70	4.95	+0.05	5.3	+0.1 <sub>0</sub>	0.19	+0.30	
pure Au		5.15	5.83						8.8

<sup>a</sup>No isomer-shift data from which to estimate  $\Delta n_s$ .

<sup>b</sup>Work-function values as estimated by A. R. Miedema except for Te (Ref. 23).

<sup>c</sup>These  $\phi$  values have been scaled from values of Ref. 23.

<sup>d</sup>Values are differences between  $AuM_2$  and the pure elements.

compound. Unfortunately,  $\phi$  values are not obtainable experimentally and are rather uncertain computationally. It has been common practice to substitute work-function values for them: work functions are a measure of the position of  $\epsilon_F$  with respect to the vacuum zero external to the crystal. In the third column of Table III are work-function values of  $\phi$  as obtained by Miedema *et al.* in their considerations<sup>23</sup> of electronegativity effects. The fourth column provides an alternate set obtained by linearly scaling the Pauling electronegativities<sup>24</sup> onto the Miedema energy scale for all elements common to the two scales. The Pauling scale, which is based on thermochemical

data, is a measure of the internal chemical potential, hence of  $\phi$ . Scaling the Pauling values in this way brings them into the energy units required here. The discrepancies between the two sets of  $\phi$  values are not altogether insignificant for estimate of site charge. Values of  $\Delta n_c$  and, where available,  $\Delta n_s$ , as based on volume corrected isomer shifts,<sup>22</sup> are also listed in Table III. Results are lacking for the  $\Delta n_s$  of Al, Ga, and In but inspection of the values for the other metalloids suggests that the assumption  $\Delta n_s = 0$  for these cases should not be far off the mark.

The unknowns  $\Delta n_p$ ,  $\Delta n_d$ , and  $\Delta \phi$  may be eliminated by solving Eqs. (5)–(8) simultaneously, obtaining

$$\delta = \frac{(\Delta E_M - \Delta E_{Au}) + (\phi_{Au} - \phi_M) + \left[ \left( \frac{dE}{dV} \Delta V \right)_{Au} - \left( \frac{dE}{dV} \Delta V \right)_M \right] - \Delta n_c [F(\text{cond}) - F(d)] + \Delta n_s (F_s - F_p)}{[F(d) - F(\text{latt})] + \frac{1}{2}(F_p - F_{latt})} \quad (9)$$

Individual terms in the numerator of this equation as well as the resulting  $\delta$  are listed in Table IV;  $\phi$  differences are based on the averages of the work function and scaled Pauling values of Table III. Equation (9) denominator terms appear in Table III. As has been noted previously,<sup>1,5,6</sup>  $\delta$  is sensitive to a competition of terms in the

TABLE IV. Terms in the numerator of Eq. (9) and the resulting net charge flow  $\delta$ .

	$\Delta E_M - \Delta E_{Au}$ (eV)	Volume terms (eV)	$-\Delta n_c [F(\text{cond}) - F(d)]$ (eV)	$\Delta n_s (F_s - F_p)$	$\phi_{Au} - \phi_M$	$\delta$
AuAl <sub>2</sub>	-0.9	+0.13	1.95	...	1.46	0.22
AuGa <sub>2</sub>	-0.8	+0.10	1.50	...	1.40	0.19
AuIn <sub>2</sub>	-0.41	+0.03	1.20	...	1.39	0.20
AuSn <sub>2</sub>	-0.52	-0.07	1.00	-0.03	1.16	0.13
AuSb <sub>2</sub>	-0.32	-0.10	0.81	-0.03	0.93	0.11
AuTe <sub>2</sub>	-0.20	-0.20	0.57	+0.07	0.67	0.08

Eq. (9) numerator. Net charge flow is always onto the Au site even though the chemical shifts alone, as indicated by the negative values of  $\Delta E_M - \Delta E_{Au}$ , would suggest charge loss. The  $\delta$  values obtained here are roughly a factor of 2 larger than those obtained previously<sup>1</sup> from the Au-site shifts only. In addition, the values vary more smoothly across the row of the Periodic Table than they did previously, and the trend in  $\delta$  is reasonable from a chemical view. It should be noted, however, that the results are sensitive to assumptions concerning Fermi-level behavior, a situation which we address in Sec. VI.

### VI. CHARGE TRANSFER AND ESTIMATES OF $\phi$

It is an often held view that  $\phi$  provides a measure of the internal chemical potential or, in other words, the electronegativity. It is further generally accepted that charge flow between two species, when they form a compound, is proportional to their electronegativity difference, that is,

$$\delta \propto \phi_A - \phi_B \quad (10)$$

This relation, while expected to hold if the two constituents are nontransition elements, may have to be modified in the case of transition metals, whose alloying behavior shows  $\Delta n_d$  and  $\Delta n_c$  to have opposite signs. It is nevertheless plausible that a series of compounds of common composition between metalloids and some transition metal, say Au, has charge transfer governed by

$$\delta = \alpha + \beta\phi_M \quad (11)$$

where  $\alpha$  and  $\beta$  are constants. Given rough estimates for  $\alpha$  and  $\beta$ , Eq. (11) can be substituted into Eq. (9) to remove the explicit dependence of  $\delta$  on  $\Delta\phi$ . By taking a set of  $\delta$  values and fitting them to a given set of  $\phi$ 's, from Table III, for example, one obtains estimates of  $\alpha$  and  $\beta$ , which in turn can be inserted into the substituted Eqs. (9) and (11) to obtain a new set of  $\delta$ . This scheme, though it converges upon iteration, does require the given set of  $\phi$ 's to fix the scale factor  $\alpha$ . Both  $\phi$  sets from Table III have been used separately and each has been used with and without the inclusion of the  $\phi_{Au}$  (and  $\delta=0$ ) in the fit. Each of these four calculations yields  $\alpha$ ,  $\beta$ , a set of  $\delta$  values, and an associated set of  $\phi$  values. The smallest range in  $\phi$  (or  $\delta$ ) is obtained in the fit using the work-function column (Table III) and omitting Au, while the largest spread results from use of the Pauling scale including Au.  $\phi$  are plotted in Fig. 4 for these two cases; the associated  $\delta$  are listed in Table V. The Pauling-based result (filled triangles) is in crude overall agreement with the two  $\phi$  sets of Table II (open and closed circles). Note that the detailed shapes of the calculated  $\phi$  results (or  $\delta$ ) are

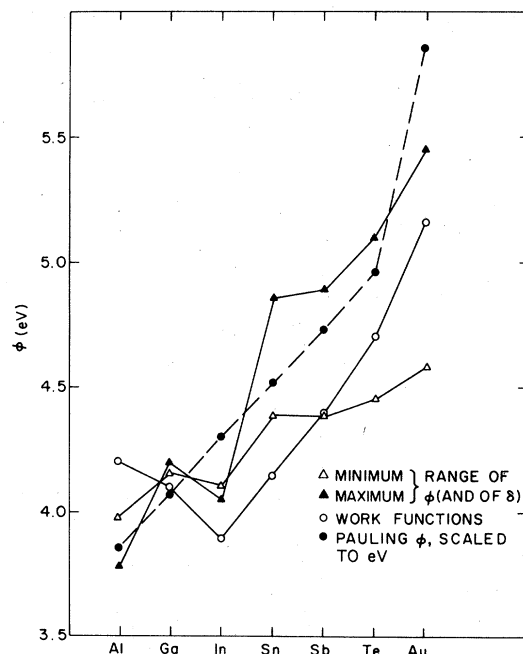


FIG. 4. Two sets of experimental chemical potentials,  $\phi$ , of the elements constituting the alloys considered in this paper. Also plotted are two independent sets of estimates of  $\phi$ : one, work functions; and two, the Pauling electronegativities expressed in eV. As discussed in the text, the two sets of experimental estimates represent the extremes of the range obtained by use of Eqs. (9) and (11).

determined essentially by the terms not involving  $\phi$  on the right-hand side of Eq. (9). The range in  $\phi$  covered by a set of solutions does indeed depend upon the given set of  $\phi$  employed in the fit of Eq. (11).

The set of "upper"-range  $\delta$  values is in quantitative agreement with the "first-pass" results of Table IV, except perhaps for AuSn<sub>2</sub>. Having arrived at the  $\delta$  values, Eqs. (5) and (7) can be used to estimate  $\Delta\phi$ ,

TABLE V. Charge flow  $\delta$  and the Fermi-level shift  $\Delta\phi$  as obtained from solutions of Eqs. (9) and (11) and from use of these  $\delta$  values in Eqs. (5) and (7). See text and Fig. 3 for the definition of  $\Delta\phi$ .

	Values based upon largest range of $\delta$		Values based upon smallest range of $\delta$	
	$\delta$	$\Delta\phi$ (eV)	$\delta$	$\Delta\phi$ (eV)
AuAl <sub>2</sub>	0.24	+0.5	0.15	+0.7
AuGa <sub>2</sub>	0.18	+0.3	0.11	0
AuIn <sub>2</sub>	0.20	+0.3	0.12	0
AuSn <sub>2</sub>	0.08	-0.7	0.05	-0.8
AuSb <sub>2</sub>	0.08	+0.2	0.05	+0.1
AuTe <sub>2</sub>	0.06	-0.2	0.03	-0.3

the position of the Fermi level of  $AuM_2$  relative to the position in the metalloid (Fig. 3). The resulting estimates are somewhat more sensitive to accumulated errors than the  $\delta$  values. In Table V the  $\Delta\phi$  are listed. Values near zero are obtained for  $AuGa_2$ ,  $AuIn_2$ , and  $AuSb_2$ ; this means that their Fermi levels are close to those of the metalloids. In the cases of  $AuAl_2$  and  $AuTe_2$ , the Fermi levels are not far from those in the metalloids.  $AuSn_2$ , however, does not fit smoothly with the behavior shown by the other compounds. Its estimated  $\Delta\phi$  value places its Fermi level substantially above those of both Au and Sn; this results directly from the fact that Au and Sn in the compound both show considerable increases in binding energy. It is interesting to note that the Mössbauer-isomer-shift Au  $\Delta n_c$  values show a break near  $AuSn_2$  as a function of varying Au-Sn composition.<sup>7</sup>

#### VII. EFFECTS OF EXTRA-ATOMIC FINAL-STATE SCREENING AND OF THE CHOICE OF LATTICE $F$ VALUES

Several matters were not considered in detail in Secs. V and VI. For example,  $F_{latt}$  and  $F(latt)$  were not defined in detail and the extra-atomic screening of the final-state core hole was not included in Eq. (9). These questions are considered below.

Electrons at the atomic site and in the surrounding medium act to screen the final-state hole charge. This lowers the final-state energy and hence reduces the binding energy. Of concern to us here is the variation in such screening on going from the pure elements to the compounds. Little is known concerning change in intra-atomic relaxation of the valence electrons on the atomic site in question, and presumably this effect is smaller than the variation of screening of the hole state charge between a good metal like Au or Al and a covalent element such as Te. It is this latter variation which should be included in Eq. (9) under the plausible assumption that Au and  $M$  benefit from the same extra-atomic screening in  $AuM_2$ . For Au, final-state screening is more important than it is in the case of Te, for example, and its effect in reducing electron binding energy is greater. These effects, if included in Eq. (11), act to increase  $\delta$  in these  $AuM_2$  systems by an amount which is greatest for  $AuTe_2$  and is small for  $AuAl_2$  where both constituents are good metals. Even in the case of  $AuTe_2$ , however, the  $\delta$  increase should not exceed  $\sim 0.09e$  and thus the sign of  $\Delta n_d$  should not be affected.

Lattice  $F$  functions are important because the atom considered in the compound is part of a structure of charged atoms which is, in total, electrically neutral. The lattice contribution to the potential of a core electron can be estimated with a spherical Madelung

sum for an ordered compound, but we have here employed a scheme<sup>1</sup> which may be applied alike to compounds and to dilute alloys. Friedel screening considerations suggest that charge removed from an atomic Wigner-Seitz cell must be quite nearby. Placing the displaced charge on a spherical shell having a radius between the Wigner-Seitz radius,  $r_{ws}$ , and  $r_{ws}$  plus one atomic unit results in a potential consistent with the Friedel picture and in numerical agreement with Madelung sums for reasonably packed structures. The  $F_{latt}$  of Sec. V were obtained assuming a charge sphere radius 1 a.u. larger than  $r_{ws}$ . Maximum values for  $F_{latt}$ , hence a minimum denominator in Eq. (9), would be obtained with a radius equal to  $r_{ws}$ . Roughly, these maximum possible values would increase the  $\delta$  values in this paper and in Ref. 1 by 20%.

#### VIII. CONCLUSIONS

We have considered quadrupole effects in the Au-Te system and the electronic structural information which may be deduced from them. We have considered also core-electron binding-energy shifts in a sequence of  $AuM_2$  compounds so that comparison could be made of charge transfer  $\delta$  among them.

As has sometimes been done, core-electron binding-energy shifts of the two sites, Au and  $M$ , were combined in order to reduce the number of assumptions required for a quantitative analysis. We have, perhaps for the first time, dealt with the Fermi-level shifts which enter the binding-energy analysis by assuming that charge transfer and the metalloid chemical potential are linearly related. Provided that this assumption is applied with a suitable set of alloys or compounds, we believe it to be at least as reasonable as the use of work functions to fix Fermi-level shifts. One may compare, as in Fig. 4, the set of chemical potential values provided by this scheme with other scales.

Values of  $\delta$  obtained in this treatment vary more smoothly through the set of compounds than did those of the earlier published work<sup>1</sup> in which Au-site shifts alone were employed. This improvement does result mainly from the use of data from both sites in Eq. (9) rather than from the effects of Eq. (11) in the fitting procedure. The new  $\delta$  values, and their associated  $\phi$ , are consonant with general conceptions of the trends of electronegativity as is seen in Fig. 4. In accord with previous observation<sup>1,4,5</sup> the  $\delta$  values are smaller in magnitude but of the same sign as the Au-site conduction-electron count changes,  $\Delta n_c$ , which have been inferred from isomer-shift data. The implication, then, is the  $d$  charge change,  $\Delta n_d$ , is of opposite sign to  $\Delta n_c$  and smaller. Au-site  $d$  charge is lost by hybridization of the  $5d$  bands with unoccupied metalloid levels. Although there is numerical



scatter in the ratios  $\Delta n_d/\Delta n_c$  they are constant within the uncertainties of the analysis.

The charge change at the metalloid site is  $-\frac{1}{2}\delta$ , which may be compared with  $\Delta n_s$  for Sn, Sb, and Te. The relative behavior of the two quantities varies smoothly across this sequence of compounds: they are roughly equal and of the same sign for  $\text{AuSn}_2$  and we estimate them to have reversed sign with respect to one another in  $\text{AuTe}_2$ . In other words, Te appears to gain  $s$ -electron count while losing net charge to Au, while in the case of Sn the charge loss is almost entirely  $s$  in character. This appears to be readily explainable. Covalently bound atoms tend to have valence  $p$  levels populated at the expense of  $s$  population; for example, elementary C, Si, and Ge have  $sp^3$  configurations, though their atomic ground states are  $s^2p^2$ . Metallic bonding, on the other hand is generally consistent with depletion in  $p$  and gain in  $s$  count relative to such covalent compounds. One would presume that the bonding of Te to Au is more metallic than the bonding of Te in its elemental form and thus Te in  $\text{AuTe}_2$  appears to exhibit an increase in valence  $s$  count despite a net loss of valence charge. In the case of  $\text{AuSn}_2$ , by way of contrast, Sn is referred to metallic white tin. Here  $\Delta n_s$  is of the same order and sign as  $-\frac{1}{2}\delta$ .

Across the sequence  $\text{AuSn}_2$ ,  $\text{AuSb}_2$ ,  $\text{AuTe}_2$  compound formation is associated with metalloid  $\Delta n_s$  values which vary from  $-0.04$  (Sn) to  $+0.05$  (Te) and corresponding  $\Delta n_p$  values varying according to Eq. (8). These  $\Delta n_s$  and  $\Delta n_p$  trends, which amount to something of the order of 0.1 electron  $s \rightarrow p$  promotion or  $p \rightarrow s$  demotion, must be of significance in relation to the heats of formation of these compounds. It may be recalled that the  $s^2p^2 \rightarrow sp^3$  promotion energy is 97 kcal/mole for carbon and it should be greater

for Sn, Sb, and Te. Thus, the roughly 0.1 electron effects in these compounds are equivalent to variations of as much as say 10 kcal/mole, an energy larger than any of their heats of formation. It should be emphasized that the  $\Delta n_s$  and  $\Delta n_p$  values derived from these experiments are at best semiquantitative; nevertheless, the present results establish that there is a promotion-demotion trend which is of energetic significance to the heats of formation of these compounds.

The quadrupole effects observed in the Au-Te system suggest that  $5d$  and " $6p$ " valence charge contribute to the quadrupole field at the Au site. There is, so to speak, an aspherical imbalance in the charge redistribution. Whether certain interstitial charge should be called Au non- $d$  or metalloid valence is academic. It would appear that this charge hybridizes with the  $5d$  bands, and contributes at the Au site to the quadrupole field and to the  $s$ - $d$  compensation.

The asymmetries in the observed quadrupole split spectra allow one to deduce the sign of the electric field gradients. The sign thus obtained here is consistent with concentration of valence electron charge density along the near-neighbor Te-Au-Te lines. This, too, is consistent with the overall picture which emerges of bonding in these compounds.

#### ACKNOWLEDGMENTS

The authors wish to thank O. C. Kistner for the loan of his Mössbauer spectrometer and W. Kunmann for preparing the alloy specimens, without which this work could not have been done. This research was performed under the auspices of the U.S. DOE.

<sup>1</sup>T. K. Sham, M. L. Perlman, and R. E. Watson, *Phys. Rev. B* **19**, 539 (1979).  
<sup>2</sup>O. Faltens and D. A. Shirley, *J. Chem. Phys.* **53**, 4249 (1970).  
<sup>3</sup>V. I. Goldanskii, E. F. Makarov, and V. V. Khar'pov, *Phys. Lett.* **3**, 344 (1963); S. V. Karyagin, *Dok. Akad. Nauk. SSSR* **140**, 1102 (1963).  
<sup>4</sup>R. E. Watson, J. Hudis, and M. L. Perlman, *Phys. Rev. B* **4**, 4139 (1971).  
<sup>5</sup>R. M. Friedman, J. Hudis, M. L. Perlman, and R. E. Watson, *Phys. Rev. B* **8**, 2433 (1973).  
<sup>6</sup>P. M. Hansen, *Constitution of Binary Alloys*, 2nd ed. (McGraw-Hill, New York, 1958).  
<sup>7</sup>J. S. Charlton and I. R. Harris, *Phys. Status Solidi* **39**, K1 (1970).  
<sup>8</sup>S. L. Ruby, H. Montgomery, and C. W. Kimball, *Phys. Rev. B* **7**, 2948 (1970).  
<sup>9</sup>C. C. Tsuei and E. Kankeleit, *Phys. Rev.* **162**, 312 (1968).  
<sup>10</sup>G. Tunell and L. Pauling, *Acta Crystallogr.* **5**, 375 (1952).

<sup>11</sup>H. L. Luo and W. Klement, Jr., *J. Chem. Phys.* **36**, 1870 (1962).  
<sup>12</sup>P. Raghavan, E. N. Kaufman, R. S. Raghavan, E. J. Ansaldo, and R. A. Naumann, *Phys. Rev. B* **13**, 2835 (1976).  
<sup>13</sup>R. Sternheimer, *Phys. Rev.* **80**, 102 (1950); R. Sternheimer and H. M. Foley, *Phys. Rev.* **102**, 731 (1956).  
<sup>14</sup>B. Perscheid, H. W. Ceyer, K. Krien, K. Freitag, J. C. Soares, E. N. Kaufmann, and R. Vianden, *Hyper. Int.* **4**, 554 (1978), and references therein.  
<sup>15</sup>We have estimated this term by placing the charge  $\delta$  evenly at the Wigner-Seitz cell boundary along the Au-Te interatomic distance. We have also placed  $\frac{1}{2}\delta$  on each of the Te atoms surrounding the Au and calculated the latter term. The results turn out to be of the order of 2% of the observed value and thus can be considered insignificant.  
<sup>16</sup>On the scale of interatomic distances in Au compounds, the free-atom  $6p$  function of Au is of substantial spatial extent. Its  $\langle r^{-3} \rangle$  value is one fifth of the value for the orbital normalized to the atomic Wigner-Seitz sphere. We

have chosen to discuss  $6p$  charge symmetry in terms of valence  $p$  charge within the atomic cell rather than in terms of charge distributed primarily on metalloid sites. This affects the conclusions one infers from Au quadrupole splittings and deserves further investigation.

- <sup>17</sup>H. Prosser, F. S. Wagner, G. Wortman, and R. Wäppling, *Hyper. Int.* **1**, 25 (1975); H. Prosser, G. Wortmann, K. Syassen, and W. B. Holzapfel, *Z. Phys. B* **24**, 7 (1976).
- <sup>18</sup>P. Flinn, S. L. Ruby, and W. L. Kehl, *Science* **143**, 1434 (1964).
- <sup>19</sup>G. M. Bancroft, K. D. Butler, and T. K. Sham, *J. Chem. Soc. Dalton* **1483** (1975); R. H. Herber, M. F. Leahy, and Y. Hazony, *J. Chem. Phys.* **12**, 5070 (1974).
- <sup>20</sup>R. N. Kuz'min, A. A. Opalenko, V. S. Shpinel', and I. A. Avenarius, *Sov. Phys. JETP* **29**, 94 (1969).
- <sup>21</sup>Taken as minus the average of the core-electron one-electron energy in the initial state and the core-hole energy in the final state.
- <sup>22</sup>Reference 1 describes the estimation of  $\Delta n_c$  and  $\Delta n_s$  based on isomer-shift data, where  $\Delta n_c$  is in terms of Au conduction electrons and  $\Delta n_s$  is for free-atom metalloid valence  $s$  electrons (being localized within the valence  $p$

shell, the valence  $s$  is, to a good approximation, described by the free-atom orbital). Unlike Ref. 1, we have estimated the effect of atomic volume change on the isomer shifts prior to extracting the  $\Delta n_s$  values. This employs volume derivatives of the isomer shift based on the experimental pressure-dependent shifts for Au [L. D. Roberts, D. O. Patterson, J. O. Thomson, and R. P. Levey, *Phys. Rev.* **179**, 656 (1969)] and for Sn [H. S. Möller, *Z. Phys.* **212**, 107 (1968)]; band-theory estimates were used to extrapolate from Sn to Sb and Te [D. L. Williamson, J. H. Dale, W. D. Josephsen, and L. D. Roberts, *Phys. Rev. B* **17**, 1015 (1978)]. The corrections have about a 10% effect on the  $\Delta n_c$ ; they are greatest for the  $\Delta n_s$  of Sb and Te, which exhibit nearly zero isomer shifts between the compounds and the elements.

- <sup>23</sup>A. R. Miedema, R. Boom, and F. R. de Boer, *J. Less Common Met.* **41**, 283 (1975). No  $\phi$  is listed for Te; this was obtained from V. S. Fomenko, *Handbook of Thermionic Properties*, edited by G. V. Samsonov (Plenum, New York, 1966).
- <sup>24</sup>L. Pauling, *The Nature of the Chemical Bond*, 3rd ed. (Cornell University, Ithaca, 1960).